Large deviations of a random walk model with emerging territories

Hendrik Schawe[1, *] and Alexander K. Hartmann[2, †]

[1]*Laboratoire de Physique Théorique et Modélisation,*
UMR-8089 CNRS, CY Cergy Paris Université, 95000 Cergy, France
[2]*Institut für Physik, Universität Oldenburg, 26111 Oldenburg, Germany*
(Dated: November 24, 2020)

We study an agent-based model of animals marking their territory and evading adversarial territory in one dimension, with respect to the distribution of the size of the resulting territories. In particular, we use sophisticated sampling methods to determine it over a large part of territory sizes, including atypically small and large configurations, which occur with probability of less than 10^{-30}. We find hints for the validity of a large deviation principle, the shape of the rate function for the right tail of the distribution and insight into the structure of atypical realizations.

I. INTRODUCTION

In ecology there is a large interest in the spatial and temporal distribution of animals. Depending on the species, the spatial distribution of individuals might be independent if they do not interact, clumped if there is some form of attraction between them, or evenly spaced for repulsive interaction of individuals [1]. Here, we are especially interested in the latter case, more specifically, we are interested in territorial species, who inhabit an exclusive territory, which is defended against members of the same species. This defense is usually either performed by aggressive behavior against intruders, or by deterrent markings of the territory, often by auditory signals or olfactory scent marks along the perimeter [1].

Central properties of interest for territories, as well as home ranges, are their size. A common method for the determination of the size and visualization of home ranges or territories is to calculate the convex hulls for the points visited in time for both experimental [2–4] as well as simulational data [5]. First studies in this directions appeared in the 1940s [6]. This sparked the interest of mathematicians, who started to work on the convex hulls of abstract sets of random points, like independently sampled points. More interesting and slightly closer to ecology are sets of correlated random points. For simple random walks, first the expectation value of the perimeter of their convex-hull was studied [7] and numerous other studies lead eventually to exact results for the stochastic properties of the area [8]. Consequently, there is quite some interest in the fundamental properties of convex hulls [9–11], but exact results concerning the full probability distributions are missing. Nevertheless, by using numerical large-deviation sampling techniques the distribution of perimeter and area of various types of random walks could be studied over hundreds of decades in probability [12–16].

Although the study of the properties of convex hulls of random points is motivated by ecological models, no study of the stochastic properties of territories, in particular when addressing the full distribution, is known to us where the set of random points originates from a more realistic model of the motion of animals. In this work, we are treating such a case based on a simple agent-based model introduced in Ref. [17], where agents perform a random walk on a lattice and leave scent marks on visited sites. When encountering a foreign scent mark, the agent backtracks away from the adversarial territory. This model gives rise to territories and with a slight modification to stable home ranges [18], i.e., the area in which an animal usually lives. Here, the size of the territory is quite straight forwardly defined as the area marked by scent and we will study the distribution of this property in very high detail using computer simulations [19]. Especially, we will explore the probability density function deep into the tails of rare events, which occur with a probability of less than 10^{-30} and identify the mechanisms leading to and the properties of such rare events of individual animals with atypically small or large territories. In particular, we will make a connection to large deviation theory and characterize the right tail of atypically large territories with an approximation of its rate function.

To obtain estimates of the probability density function for the size of territories with such a high precision, we need to employ Markov chain Monte Carlo importance sampling methods, which we will describe after a precise model description in Sec. II. Then, in Sec. III, we will show and interpret the results of our simulations. Finally we summarize our findings in Sec. IV.

II. MODELS AND METHODS

A. Model Specification

We are studying a model for the emergence of territory by scent marks introduced in Ref. [17]. This model lives in discrete d dimensional space. At time $t = 0$ there are M agents starting uniformly randomly distributed on sites of a lattice under the condition that no two agents start on the same site. The lattice has L^d sites and

---

* hendrik.schawe@cyu.fr
† a.hartmann@uol.de

periodic boundary conditions, which we call the *world*. On this lattice, there is a discrete-time dynamics and we are interested in the state at time T. At each of the $t = 1, \ldots, T$ time steps, all agents move synchronously to one of the $2d$ adjacent sites. At each time step each agent marks the current site with its individual scent, potentially adding a new scent to already existing scents. The way the adjacent site is selected, is determined by the scents on the current site at time t. If there is no scent of other agents on the current site, the agent visits at time $t+1$ a uniformly randomly selected adjacent site. Otherwise, if there is an adversarial scent, the agent has to step at time $t+1$ on an adjacent site already marked with its own scent, i.e., it backtracks into its own territory. Note that the site from which the agent retreats, was marked also with its own scent on entering at time t. A scent stays active for t_a time steps. For $t_a = 0$ this corresponds to non-interacting agents, each performing a standard random walk on a lattice, and $t_a = T$ to static territories. Values in between allow the territories to move on a slower time scale as demonstrated in Ref. [17]. In this study, we will concentrate on the $t_a = T$ edge case of permanent scents, which never evaporate.
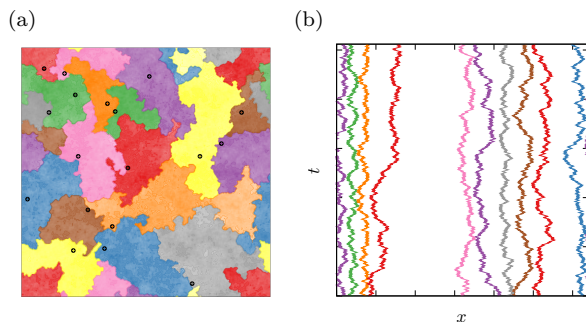

FIG. 1. Example for the (a) $d = 2$ case of $M = 18$ agents on a world with periodic boundaries of size $L = 256$ after $T = 5 \cdot 10^6$ time steps. The intensity and the contour lines show how often a site was visited by an agent, the markers show the initial positions. Note that there are only 9 colors and each is assigned to two unrelated agents; and (b) for the $d = 1$ case with $M = 10$, $L = 320$ after $T = 1024$ steps. Territory of the black agent 0 is marked as the distance ℓ below the horizontal axis; the distance Δ is the possible space available between the starting positions of agent 0's neighbors.

The interpretation of this model for $d = 2$ is quite intuitive, as there are two dimensional territories of marked regions arising, if the density of agents is sufficiently large. In the case of a site marked by several individuals, it is considered as being part of the territory of every agent with an active scent on the site. In Fig. 1(a) an example is shown where each field is colored with an agent specific color whose intensity depends on the number of visits to the corresponding site (and additional contour lines for clarity). Clearly, the dynamics lead to extremely well defined territories.

However, also the $d = 1$ version of this model has di-

rect application, e.g., Ref. [17] uses it to model organisms which actively refresh the scent marks on the perimeter of their territory, and compares it with empirical data obtained from foxes. The rationale to use the one dimensional version of this model is that a $d = 1$ agent hitting the border of its territory and refreshing the scent mark on one site of a line is similar to a $d = 2$ agent walking directly along half of the perimeter of its territory—an event which can not be modeled with a random walker in two dimensions.

Since the main mechanism of this model is the interaction of multiple agents, we have to carefully determine the size of the world: too large and there will not be any interaction, too small and agents will be restricted to a handful of sites. Especially, we need to pay attention how the size of the world should scale with increasing number M of agents or larger number T of steps. Since the single agents behave in a diffusive way, we scale the size of the world as $L = \lfloor a \sqrt[d]{M} \sqrt{T} \rfloor$, where a is a free parameter to determine the density of agents. Since a is an inverse density we will call it *sparsity*. This leads to a roughly similar number of interactions between agents when increasing M or T, which we checked numerically (not shown). To clarify, consider a scaling of the world size proportional to T, which would fundamentally change the behavior from a crowded world for small values of T to free diffusion without any interaction for large values of T.

In the following we will only study the $d = 1$ case, although all methods work in principle in arbitrary dimensions. The observable, we are studying is the total size ℓ_i of the territory of agent i, i.e., the number of sites marked with the corresponding agent's scent. We will mostly concentrate on one arbitrarily chosen "agent 0", without loss of generality. Its territory will be denoted as ℓ without subscript. In particular, we are interested in rare territories, which are much larger or smaller than typical territories, but which only occur very rarely, e.g., when a single agent claims almost the whole worlds as its territory. If one wants to obtain such events over a substantial range of the distribution's support, we need to generate events with probabilities a small as 10^{-30}. This requires the application of sophisticated algorithms, which we explain next.

B. Sampling Rare Events

To characterize these extremely rare events, we will look at the the *rate function* $\Phi(\ell/T)$, which is a central element of *large deviation theory* [20]. It describes the behavior of a large class of distributions in the limit of, in this case, large times T. Here we will test it for the distribution of territory sizes after T steps $P_T(\ell)$. The rate function is defined for our case by

$$P_T(\ell) = e^{-T\Phi(\ell/T) + o(T)}. \tag{1}$$

If the distribution $P_T(\ell)$ can be described in such a way using a rate function, one says the distribution fulfills a

large deviation principle. Note that Φ is a function of ℓ/T, i.e., the ratio of the territory size ℓ to the maximum size which is possible after T steps. This also means that, although the full probability distribution is described by Eq. 1, the region of typical events with a finite probability, say $P_T(\ell) > 10^{-10}$ shrinks to a width of zero on the x-axis as $T \to \infty$.

Here we want to approximate the rate function Φ valid for $T \to \infty$ using simulations of systems with finite values of T. From the distributions of finite sizes $P_T(\ell)$ we can calculate *empirical* rate functions Φ_T.

There are cases where the probability density does not follow Eq. 1 but can still be expressed by

$$P_T(\ell) = e^{-T^\alpha \widetilde{\Phi}(\ell/T) + o(T^\alpha)}. \tag{2}$$

for some exponent α, which may even differ for the left and right tail [21]. Since our data shows that the right tail $\ell \gg \langle \ell \rangle$ follows this form with the classical $\alpha = 1$, but the left tail $\ell \ll \langle \ell \rangle$ does not, we will focus our evaluation on this part.

Since the empirical rate functions converge towards a limiting form for $\ell \gg \langle \ell \rangle$, as we will see in Section III, we can even use them to estimate an approximation of the functional form of the right tail behavior $\Phi^{(r)}$. We will indeed observe a functional form of $\Phi^{(r)}$ very similar to standard random walks.

Obtaining the data of the far tails of the distribution $P(\ell)$, needed to calculate the empirical rate functions, is far from trivial. The conventional method of generating independent samples, generating a histogram from them and estimate the distribution from that, is limited to values of ℓ which have a large probability to be observed during a feasible simulation time, say, larger than 10^{-10}. But probabilities of 10^{-30}, which might be needed to characterize the far tails, are far beyond reach of this method.

To sample events with such low probabilities efficiently, we resort to a Markov chain Monte Carlo (MCMC) method, which was used previously for a range of different applications [22–24] including the study of areas of convex hulls enclosing the traces of random walks [12, 13, 15]. Since the method has been described elsewhere, we only give a brief description here, which mainly defines the actual implementation for the present model and few general explanations. For our MCMC approach, the *states* of the Markov chains are given by a *realization* of the set of M random walks. Thus, each state consists of a stochastic simulation itself, of the actual random walks, and the random walks are embedded into a higher-level Markov chain.

First, as for any Markov chain method with the Metropolis-Hastings algorithm [25], we have to define a *change move* to generate trial realizations. While there are elaborate and efficient change moves for the simple random walk or the self-avoiding random walk used for polymer simulations [26], we are not aware of any prior work for the mutually-avoiding random walks of the territoriality model we study. The growth mechanism of

the territoriality model does indeed prevent the use of methods similar to the ones used for the mentioned non-growing random walk models, (which is explained in a bit more detail in [15]). Therefore we resort to a method which does not operate on the random walk itself, but on the random numbers used by the computer program to generate the random walk. This method was introduced to study non-equilibrium processes in Ref. [27] and successfully applied to different models defined by growth processes [15, 16, 23]. To understand the approach, note that for any stochastic simulation it is necessary to construct a realization of the studied ensemble from a sequence of random numbers. Clearly, it does not change the behavior if one first generates all the random numbers, stores them in a vector $\xi = (\xi_1 \ldots, \xi_K)$, and uses them for the actual stochastic simulation, i.e., to construct the random walks. In this way, a realization of the stochastic simulations, the set of generated random walks here, depends deterministically on ξ. Thus, a realization and the vector ξ can be used synonymously. Instead of constructing the Markov chain from realizations and propose change moves applied to the realizations, we build a Markov chain $\xi^{(0)} \to \xi^{(1)} \to \xi^{(2)} \to \ldots$ consisting of random number vectors as states and apply change moves to these vectors. This requires a lot of computational power, because generally after each change move a new realization of M random walks has to be constructed from a vector ξ. But this approach is quite generally applicable to models, for which specialized change moves on the realizations are not trivial to construct.

In this concrete case, the random number vector consists of $K = M + MT$ random numbers uniformly distributed between 0 and 1. The first M entries are used to determine the initial positions, which are uniformly distributed on a lattice under the constraint that no site might start with two agents. The latter MT random number entries are used to determine for each of the M agents at each of the T timesteps which site to visit next under the constraint of the rules introduced in the previous section. A change move selects a random entry of the vector ξ and replaces it by a new uniform random number. The interpretation of each random number depends on the realization: if the current site has no adversarial scent, it is used to decide on which of the $2d$ neighboring sites to step; otherwise it is used to decide on which of the usually far fewer adjacent sites of its own territory to step. This necessitates that for each given random vector ξ the random walk simulation has to be performed from the beginning again: a change, which makes an agent step left instead of right at timestep t, might influence its left neighbor who has to retreat at $t + 2$ instead of stepping right. In two dimensions, one could easily imagine that such a change could influence the configuration heavily, e.g., by closing a 'passage' between two territories, trapping a third agent. Note that such large changes in ℓ from changes proposed to the MCMC algorithm usually lead to a decreased performance. As we will explain in a few paragraphs, this cascading effect contributes to our

decision to study the one-dimensional case.

For the Metropolis-Hastings algorithm the change moves will either be accepted, i.e., used as the next state of the Markov process, or rejected, i.e., the current state is kept, according to the Metropolis acceptance probability [28]

$$p_{\text{acc}} = \min\left\{1, e^{-\Delta E/\Theta}\right\}. \tag{3}$$

Here Θ is an artificial temperature, whose role will be explained in the next paragraph. We identify the "energy" E with our observable of interest, which is obtained from each realization of the random walks, here $E \equiv \ell$, and $\Delta E = E(\xi') - E(\xi)$ denotes the change in this quantity between the current realization given by the current vector ξ and the proposed trial realization ξ'.

We can choose the artificial "temperature" Θ freely, especially—in contrast to natural temperatures—it can also assume negative values. Note that this means that small positive values of the the temperature will reject most changes which increase ℓ, and therefore lead to atypically small territories. On the other hand, small negative values of Θ will reject most changes decreasing ℓ, such that the encountered realizations will have atypically large areas. Large values of Θ, regardless the sign, will accept almost all changes and therefore generate typical realizations. Indeed we can be more precise how exactly the encountered realizations ξ will be distributed with respect to ℓ. They will eventually be distributed according to the Boltzmann distribution

$$Q_\Theta(\xi) = \frac{e^{-\ell/\Theta}}{Z(\Theta)}Q(\xi), \tag{4}$$

where $Q(\xi)$ is the distribution of random vectors, i.e., effectively realizations of random walks, one would encounter when simply sampling from the territorial model and $Z(\Theta) = \sum_\xi e^{-\ell(\xi)/\Theta}Q(\xi)$ the partition function, which just takes the role of a normalization constant for our purposes. Conveniently, we can calculate the distribution $P(\ell)$ from the distribution of realizations by summing the probabilities of all realizations with the same value of ℓ and analogously for the distribution $P_\Theta(\ell)$ measured in the biased Markov chain, which leads with Eq. (4) to the following identity [22]

$$\begin{aligned}P_\Theta(\ell) &= \sum_{\{\xi|\ell(\xi)=\ell\}} Q_\Theta(\xi) \\ &= \sum_{\{\xi|\ell(\xi)=\ell\}} \frac{1}{Z(\Theta)} e^{-\ell(\xi)/\Theta} Q(\xi) \\ &= \frac{1}{Z(\Theta)} e^{-\ell/\Theta} P(\ell), \end{aligned} \tag{5}$$

which we can use to remove the bias from our measured $P_\Theta(\ell)$, to obtain the distribution $P(\ell)$ of the original territoriality model.

The last ingredient missing is the knowledge of $Z(\Theta)$, which we can obtain by exploiting the uniqueness of $P(\ell)$,

i.e., if we have estimates for two biased distributions at different values of the artificial temperature $P_{\Theta_i}(\ell)$ and $P_{\Theta_j}(\ell)$, we can calculate the ratio of the two corresponding $Z(\Theta_i)$ via

$$e^{\ell/\Theta_i} Z(\Theta_i) P_{\Theta_i}(\ell) = P(\ell) = e^{\ell/\Theta_j} Z(\Theta_j) P_{\Theta_j}(\ell). \tag{6}$$

This requires us to obtain estimates for biased distributions at multiple values of the artificial temperature, such that they overlap pairwise. Also the statistical precision of the estimate in the overlapping region should be decent to avoid large statistical uncertainties. As alluded to before, we can tune the typical values of the territory size ℓ encountered in the Markov chain with careful choices of Θ, such that the encountered values of ℓ show sufficient overlaps. Note that when increasing the system size, i.e., the number K of entries of ξ, one has to increase the number of different values of the temperatures Θ in order to cover a substantial range of the support of $P(\ell)$. Here, we used up to 14 different temperatures. Note that the simulations for different artificial temperatures are completely independent and can be performed in parallel.

As for all Markov chain Monte Carlo techniques, the subsequent realizations in the Markov chain are correlated. So one has to ensure that the Markov process is in equilibrium before taking measurements and to perform enough change moves before taking the next measurements to allow the samples to decorrelate [25].

This sampling method also allows us to measure other properties of the encountered samples. While a full joint probability distribution would need two independent artificial temperatures and much more simulation time, we can use the values of a second observable o encountered during one simulation, to construct a partial joint probability distribution using Bayes' theorem. Because ℓ is biased, the pairs (o, ℓ) encountered during the simulation can not be used to estimate the joint probability $P(o, \ell)$ directly, but they can be used to estimate the conditioned probability $P(o|\ell)$. After the simulation we obtain $P(\ell)$ from the data, as described above. Now Bayes' theorem allows us to obtain a part of the joint probability density $P(o, \ell) = P(o|\ell)P(\ell)$.

Markov chain Monte Carlo methods are still rather compute intensive and a systematic study of the two-dimensional territories is infeasible, as we explain now: It necessitates a number of agents M which increases quadratically in the linear size of the system to preserve a fixed sparsity. The linear size of the system must be larger than T to avoid extreme walks to interact with themselves (or for non-periodic borders with the boundary). At the same time the interaction between the different agents leads to a problem when choosing the change moves: A single changed step of a single agent will cascade via the interactions through the whole system and often introduce a substantial change, which has to be rejected. This is aggravated by the fact that quite large times T are necessary to observe the formation of territories. Since current studies of the full distribution of home

range areas for comparable random walk models with a single random walker are limited to $T < 10000$ [12–15], even though there exist efficient change moves for those models, the two-dimensional case of the territory model is beyond reach at the moment.

Fortunately, the problems of the two-dimensional case either vanish or are far less severe in the one-dimensional case. In one dimension agents can not go beyond the initial positions of their direct neighbors, such that the linear size may be smaller than T without risking self-interaction. This also reduces the severity of the cascading of change moves through the whole systems, since mostly only the two direct neighbors will be affected. Finally, the number of agents M scales only linear in the linear size of the system to preserve a fixed sparsity, instead of quadratically. Therefore, we will present in the following sections our numerical results characterizing the one-dimensional case and compare them to a standard random walk on the same lattice (the $M = 1$ case).

III. RESULTS

Before we dive into the full distribution, it is useful to take a look at the behavior of the mean territory size $\langle \ell \rangle$. This can be obtained via simple sampling, such that we have access to larger systems than for the study of the full distribution.

One of the fundamental properties of simple random walks is their diffusive behavior, i.e., observables characterizing their size along one dimension scale as $\sqrt{T}$ in the number of steps, i.e., $\langle \ell \rangle / \sqrt{T} \to \mu$, for $T \to \infty$ where μ is a constant. We expect this for the present model as well, which is reflected by the scaling of the world size like $\sqrt{T}$. Our results shown below are consistent with that. Also the value of μ and its dependence on a or M are still of interest.

Therefore we show in Fig. 2 the average territory size $\overline{\ell}$ measured over 10^6 random realizations for different numbers of steps taken T and different values of the parameters determining the number M and sparsity a of agents. Here we choose intermediate values of a, since very large ones would inhibit the interaction between the agents. The solid lines are fits to the form $\ell = \mu\sqrt{T} + C_1$, where the first term mirrors the dominating diffusive scaling behavior and the second term should account for corrections to this scaling for finite sizes.

Indeed, the fits of this form describe the behavior well (with χ^2_{red} goodness of fit values between 0.7 and 1.2 for all shown cases.) The fit results for C_1 are always smaller than 0.5, i.e., they have no visual impact on Fig. 2. The values of μ obtained by the fits are listed in the caption of Fig. 2 and are much smaller than the known value of the *span* of simple random walks. The span is the distance from the leftmost to rightmost visited point, which is analogue to our territory. For a one-dimensional lattice with unit spacing it is known to be $\mu = \sqrt{8/\pi} = 1.596..$

[29], i.e., the interaction of the agents has a large influence on the *typical* behavior.
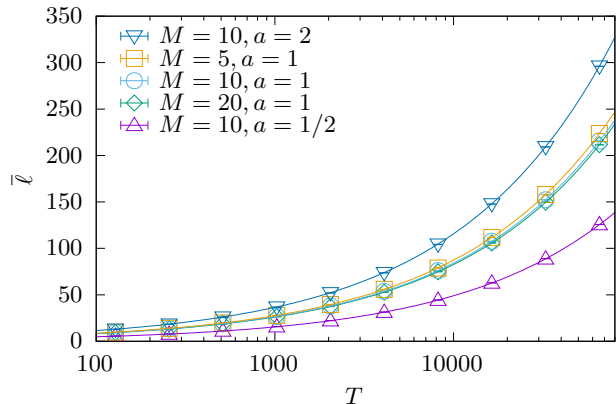

FIG. 2. Behavior of the mean territory size for a selection of parameters M and a. The horizontal axis is shown with a logarithmic scale to adequately show the measured values over many orders of magnitudes. Fits are to $\ell = \mu_{M,a}\sqrt{T} + C_1$ for $\ell \geq 1024$. The resulting values are $\mu_{5,1} = 0.8737(3)$, $\mu_{10,1/2} = 0.4905(2)$, $\mu_{10,1} = 0.8418(3)$, $\mu_{10,2} = 1.1572(3)$, and $\mu_{20,1} = 0.8272(3)$.

Interestingly the choice of the number of agents M, despite not changing the sparsity of the agents, has an influence on the asymptotic territory size, as the value of μ decreases with growing value of M. Since we do not look at any special agent, this must mean that more agents lead to a higher proportion of unclaimed territory. Less surprising is that a increased sparsity a, i.e., lower density of agents, does not lead to proportionally more territory. Especially for large values of the sparsity a, the limiting factor is not the amount of unclaimed territory, but the diffusive behavior of the agents which have access to the largest area of free territory, while other agents are restricted to small areas due to unfavorable initial conditions. This effect, however should diminish greatly in the two-dimensional version of the model.

For standard random walks without territorial competition it is well known that not only the means but the whole distribution of the span shows a T-independent form when scaled with $\sqrt{T}$ [30, 31]. If this scaling is also valid for the territoriality model under scrutiny, we would expect that the distributions measured for different values of the number of steps T would collapse on the same T-independent scaling form, i.e.,

$$\widetilde{P}(\ell/\sqrt{T}) = \sqrt{T}P_T(\ell). \tag{7}$$

In the inset of Fig. 3 we can see that this collapse works well in the high-probability region. Also there is a comparison to the distribution $P(\ell)$ of a simple random walk on a lattice, which has its maximum at larger values of $\ell/\sqrt{T}$, which is consistent with our results for the mean values, from above. In the main plot of Fig. 3, we can observe the same effect over almost the whole distribution.

Only in the far right tail, where effects of the finite-size world come into play, deviations from the common curve are strong.
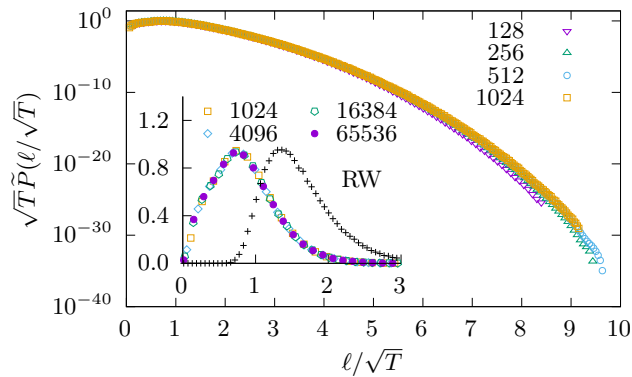

FIG. 3. Distribution of the territory size $P_T(\ell)$ for different numbers of steps $T \in \{128, 256, 512, 1024\}$ including very rare configurations. The axes are scaled to collapse all sizes on a size-independent scaling form. The inset shows the high probability part with a linear instead of logarithmical axis with data obtained via simple sampling and therefore larger values of $T \in \{1024, 4096, 16384, 65536\}$. Also shown is a standard random walk (RW) for comparison. Not all available data points are shown for clarity.

To study the far tails of extremely rare configurations in more detail, it is useful to look at examples of such rare instances. In Fig. 4 examples for both the left and right tail are shown. They are realizations from the equilibrium distribution of the artificial temperature ensemble at $\Theta = 1$ and $\Theta = -1$ respectively.
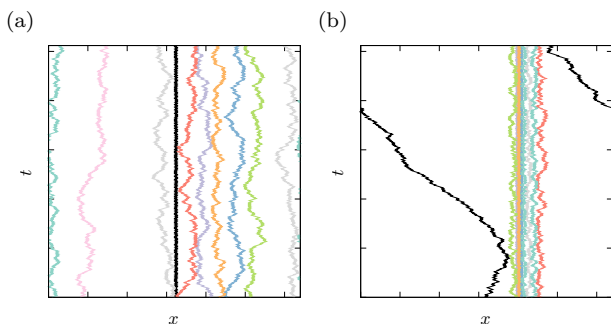

FIG. 4. Example configurations with a number $T = 1024$ of steps, world size $L = 320$, and a number $M = 10$ of agents obtained where agent 0 (black lines) is biased to (a) small territories and (b) large territories. Apparently a large contribution to the territory an agent can annex, depends on the initial positions, either confining the agent, resulting in very small territories, or confining most other agents, resulting in a very large territory. In the latter case, also a rare configuration of steps taken is necessary to achieve the observed ballistic movement leading to a large territory.

First, consider Fig. 4(a) corresponding to a realization from the left tail. Apparently agent 0, marked in black, is confined from the very beginning by its two neighbors which start extremely close to each other. All other agents seem to behave quite typically. If we assume that this trapping mechanism is the dominant mechanism leading to very small territory sizes ℓ, we can try to estimate the behavior of the left tail of the distribution. Therefore we need to know the distribution of the distance Δ from the left to the right neighbor of agent 0. Since the starting positions are almost independent (the only correlation arises by the impossibility of two walkers starting on the same site), we can approximate the initial positions as a Poisson point process. Note that the Poisson point process lives on a continuum, while we have a discrete lattice. Therefore the approximation becomes better for increasing size of the world L. Fortunately, for a Poisson point process with a point density of, here, $\lambda = M/L$ the distribution of the size δ of Voronoi cells, i.e., half the distance $\Delta = 2\delta$ to the left and right nearest neighbors, is known to be $P(\delta) = 4\lambda^2 \delta e^{-2\lambda\delta}$ [32].

For small values of Δ the diffusion of the agent would cover all of the available area. Due to the competition of its adversaries we would expect that for a given (small) value of Δ an area of $\Delta/2 = \delta$ would be claimed by agent 0 on average. Thus we use $\delta \approx \ell$ and expect

$$P_T(\ell) \approx 4\lambda^2 \ell e^{-2\lambda\ell} \qquad (8)$$

for small values of ℓ. We compare this approximation to the data we simulated in double logarithmic axes to emphasize the left tail. We rescale the axes the same way as in Fig. 3, to enable the visualization of very different sizes in the same plot. Also, this scaling lets Eq. (8) collapse on a T-independent scaling form. Note that the events in the left tail are probable enough that we can observe the whole tail using our simple sampling results: they often reach the very leftmost point $\ell = 2$ of minimal possible territory in this model. First, we can see in Fig. 5 a reasonable matching, with a deviation of 20% over most of the tail, between our measurements and the approximation. The matching becomes better for larger values of T, which is expected, since the approximation Eq. (8) becomes better in that case. Thus, the initial positions of the agents determine the left tail of the distribution of territories in a major way. We will explore this in more detail using correlations of multiple observables later in this manuscript.

For the right tail of larger than typical territories the instances seem to consist of extremely dense initial conditions for all agents, in such a way that the agent with the largest territory can occupy almost the whole world, which is shown in Fig. 4(b). The total size of the territory should therefore depend somewhat on the size of the world. However, the "straight line" movement in the example suggests a ballistic character of the agents with extremely large territories, i.e., for extremely large territories, additionally to the rare initial conditions, also a rare configuration of steps is necessary. In this case the territory size ℓ should scale like the number of steps T in the far right tail for worlds which are large enough.
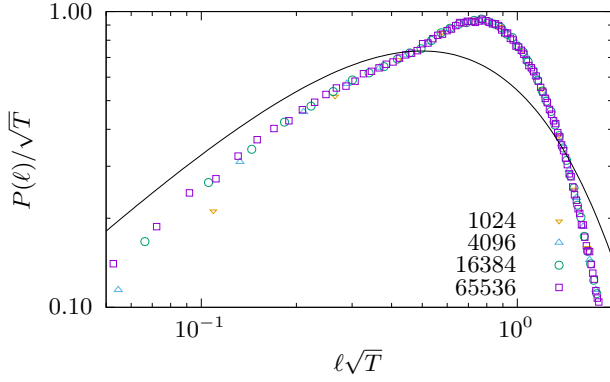
FIG. 5. Rescaled probability densities $P_T(\ell)$ in a log-log plot to emphasize the left tail for walks with different number of steps T. The solid line is the distribution (8). The size of the world scales as $L = \lfloor aM\sqrt{T} \rfloor$ with $M = 10$ agents and sparsity $a = 1$.
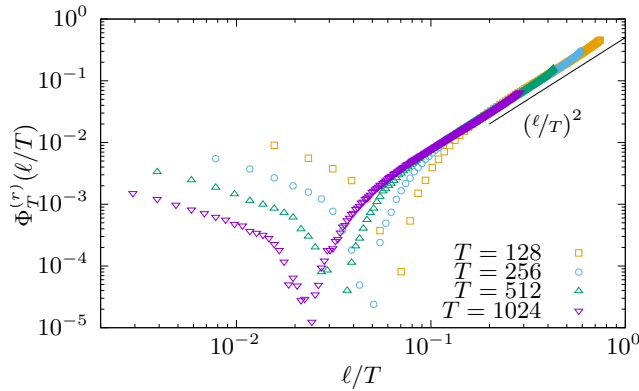

FIG. 6. Empirical rate functions in a log-log plot to emphasize the power-law behavior of the right tail for walks with different number of steps T. The size of the world scales as $L = \lfloor aM\sqrt{T} \rfloor$ with $M = 10$ agents and sparsity $a = 1$.

Therefore, we scale the horizontal axis of the rate function like ℓ/T in Fig. 6, i.e.,

$$P_T(\ell) \approx e^{-T\Phi^{(r)}(\ell/T)}. \tag{9}$$

Further we shift all empirical rate functions such that their minimum has a value of zero. Note that this is a property of the rate function, because the probability should not converge to zero for exactly every value of ℓ. The shift does therefore not change the form to which the empirical rate functions converge with increasing T. Indeed, for our data we observe that the right tails converge to a common form, which behaves like $\Phi^{(r)} \propto (\ell/T)^2$ until effects of the limited world size and therefore limited territory size truncate the distribution. This is the same behavior of the rate function as for a single random walk observed before [12, 14]. Assuming the rate function behaves like a power law for large values of T in the right tail, $\Phi_T^{(r)}(\ell/T) \to (\ell/T)^\kappa$, one can understand the value

of the exponent $\kappa = 2$ by comparing the form of the distribution expressed via the rate function in Eq. (9) with the scaling Eq. (7) demonstrated in Fig. 3. Since this should only be valid for large values of T, we can neglect the $\sqrt{T}$ factor in Eq. (7) and arrive at

$$\exp\left(-T\Phi^{(r)}(\ell/T)\right) \approx \widetilde{P}\left(\ell/\sqrt{T}\right) \tag{10}$$

Since $\widetilde{P}$ has no explicit dependency on T, we must be able to formulate the left hand side as a function of the same argument $\ell/\sqrt{T}$:

$$\exp\left(-T\Phi^{(r)}(\ell/T)\right) \approx \exp\left(-T(\ell/T)^\kappa\right) \tag{11}$$

$$= \exp\left(-\left(\ell/T^{(\kappa-1)/\kappa}\right)^\kappa\right) \tag{12}$$

and therefore $(\kappa - 1)/\kappa = 1/2 \Rightarrow \kappa = 2$. Note that this argument is more generally stated in Ref. [15]. One can observe a collapse onto a common curve for the right tail onto this form, which suggests that the large deviation principle holds here and no fundamental differences to standard random walks exist for the limit of extremely large territories—though the detailed shape and location of the typical region differ a lot (cf. Fig. 3).

In the almost complete probability density functions we showed, it is obvious that very large territory sizes are far more rare than very small territory sizes. This can be made plausible by the following simple argument: While left-tail events only need two arbitrary agents to start close to agent 0, right tail events need every agent to start in a very small region. Also while left tail events do not need any rare configuration of steps, since the starting positions are already sufficient to restrict agent 0 to a very small territory, right tail events need a rare configuration of steps from agent 0, to span the available territory. For extremely right-tail events, even the neighbors need to show rare subdiffusive behavior to not claim territory before agent 0 arrives.

Although, we limited this study to the limit $t_a = T$ of permanent scents, there are still free parameters like the sparsity a and number of agents M. We will test their influence on the full distribution with a very short parameter study shown in Fig. 7.

First, we should consider the influence we expect for different values of the sparsity a: Since a directly governs the density of agents due to $L \propto a$, one would expect for small values of the sparsity a, i.e., high densities, that the distribution $P(\ell)$ becomes concentrated around the minimum $\ell = 2$. For large values of a, the density decreases so far as to prohibit interactions between agents, such that the territory size ℓ will behave the same way as the span of a single random walk. Both expectations are met when looking at the inset of Fig. 7(a). Here for smaller values of a a more pronounced peak at lower values of ℓ arises and the curve for larger values of a becomes more similar to the curve of a single random walk shown as a black line. Moreover, the main plot shows the behavior of the tails. Here, a truncation effect becomes visible, as the
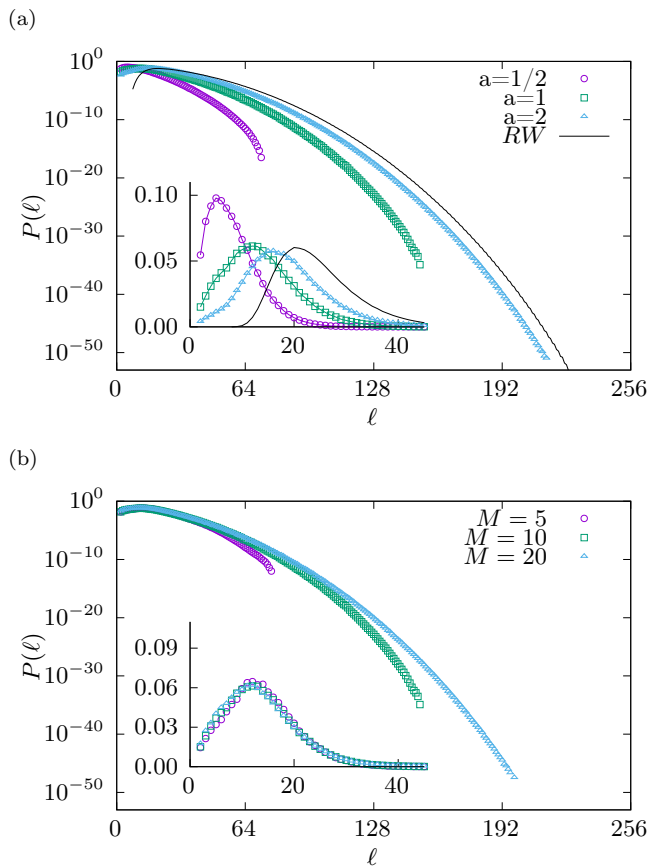
FIG. 7. Parameter study. $L = \lfloor aM\sqrt{T} \rfloor$. (a) varying a ($M = 10, T = 256$), lines visualize a standard random walk (RW), (b) varying M ($a = 1, T = 256$). The $M = 10, a = 1$ data set is the same as shown in Figs. 3 and 6 for $T = 256$.

M.

Previously, we considered a few extreme example configurations to get a feeling for the structure of extreme configurations. To get a more complete and quantitative picture, we can instead scrutinize the joint probability of two characteristic observables. From the data collected during the necessary simulations for determining $P(\ell)$, using Bayes' theorem as described in Sec. II, we can determine very large parts of the joint probabilities of ℓ and any observable, as shown in Fig. 8, for very little additional computational cost.
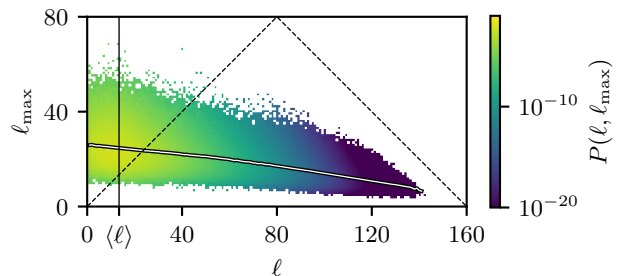

FIG. 8. Joint probability distribution of $P(\ell, \ell_{\max})$ showing anti-correlation of the size of the territory of agent 0 with the largest territory of its adversaries for $T = 256$, $M = 10$, $a = 1$, $L = 160$. The dashed lines mark $\ell_{\max} = \ell$ (rising), $\ell_{\max} + \ell = L$ (descending). The vertical line shows the mean value $\langle\ell\rangle$ and the white line with black outline the average of $\ell_{\max}$ restricted to the given value of ℓ.

First, we show in Fig. 8 the joint probability of ℓ and the size of the largest territory of all other agents $\ell_{\max} := \max_{i>0}\ell_i$. Parts of the joint distribution are marked white, if there are no data. Note that the upper right triangle above the dashed line has a probability of 0, since the sum of the two territories must be smaller or equal to the size of the world, also the $M-2$ other agents block at least a small territory. The white line with black outline shows the mean values $\overline{\ell_{\max}}(\ell)$ for each value of ℓ, it exhibits an expected slight anti-correlation. This anti-correlation is due to the fact that all agents share the same world, if one occupies more, the others get less. The distribution can be split into two parts, one where the territory of agent 0 is dominating, below the line given by $\ell_{\max} = \ell$, and another where one of the other agents covers the largest territory, above this line. In the region where agent 0 has a territory of typical size, marked by the vertical line, almost always at least one other agent covers a larger territory. The distribution is located in the figure above the rising dashed line. In particular one can learn from this figure that only when agent 0 covers about twice of its typical territory, where the rising dashed line crosses the $\overline{\ell_{\max}}(\ell)$ line near $\ell = 25$, agent 0 covers among all agents the largest part of the world. This is where the real large-deviation behavior sets in.

Next, in Fig. 9, we want to study the efficiency of the agents. Here again we mark the inaccessible region in the

world size L becomes smaller than the number of steps T and the extremely large territories do not fit into the world anymore. However, for fixed, non-zero values of a, we expect the $T \to \infty$ limit of the right tail rate function $\Phi(\ell/T)^{(r)}$ to exhibit the same $(\ell/T)^2$ shape, which we observed for $a = 1$ before and for the non-interacting limit $a \to \infty$ in [12, 14, 15], with possible differences in the prefactor.

Next, consider the influence of the number of agents M. Since the density of agents is independent of M, due to the scaling of $L \propto M$, we do not expect a large influence of M on the typical regime beyond the slight influence we already observed for the mean value in Fig. 2. While very low values of M, like $M = 2$ will surely impact the interaction between the walkers, this effect should diminish quickly for larger values. Indeed, the distribution $P(\ell)$ for $M \geq 5$, which we visualized in the inset of Fig. 7(b), are very similar to each other. However, for the far tails visualized in the main plot, considerable differences become apparent. Since $L \propto M$, we encounter the same truncation as visible for small a. So larger values of M allow us to explore deeper into the right tail—unfortunately the computational cost also increases with

top right of the diagram by a dashed line. Also here, the conditioned mean at a given value of the territory size ℓ is indicated by a white line with black border.
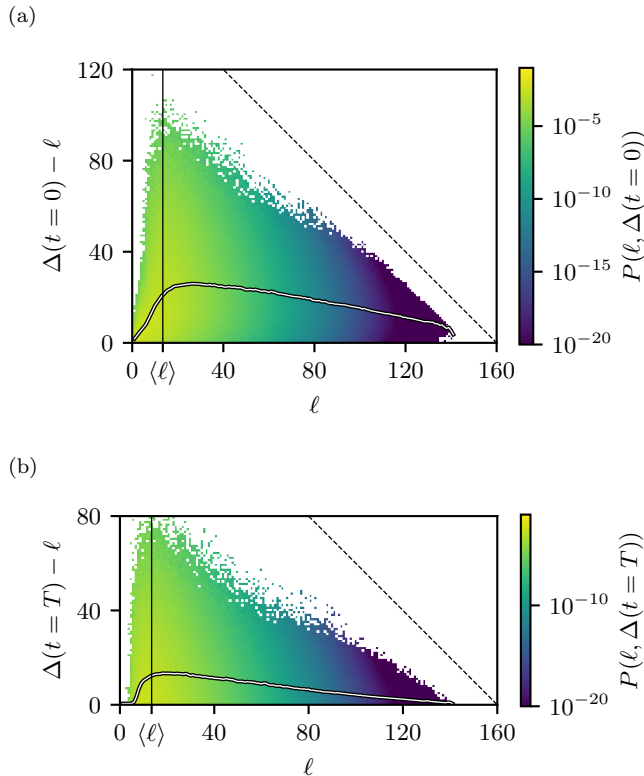
(a)

(b)

FIG. 9. Joint probability distribution of $P(\ell, \Delta)$ showing correlation of the size of the territory of agent 0 with (a) the distance $\Delta(t = 0)$ between its initial neighbors and (b) the distance between the final territories of its neighbors $\Delta(t = T)$ for $T = 256$, $M = 10$, $a = 1$, $L = 160$. The vertical lines again show the mean value $\langle \ell \rangle$ and the white lines with black outline the average of $\Delta(t = 0) - \ell$, respectively $\Delta(t = T) - \ell$, restricted to the given value of ℓ.

First, in Fig. 9(a) we look at the observable $\Delta(t = 0) - \ell$, which is how many sites, of those which are accessible given the starting positions, are not claimed. This is a measure of inefficiency. Since lower values of $\Delta(t = 0) - \ell$ signify a more efficient use of the available space, we encounter the—only at the first sight—counter-intuitive result, that agents with exceptionally small territories are still exceptionally efficient. This can be explained by the fact that the initial positions are indeed the driving factor resulting in very small territories. Also note that at very small values of ℓ we encountered no realizations with even typical values of Δ, shown by the large white area for small values of ℓ. Also we note that for small values of ℓ the mean of $\Delta(t = 0) - \ell$ has a slope of almost one, which supports our guess that in this case the agent should claim on average half of the initially available space. The maximum of this inefficiency measure is reached around the typical realizations of $\ell \approx \mu \cdot \sqrt{T}$ ($\ell \approx 13.4$ for these data). To reach larger than typical territory sizes, the

inefficiency has to decrease again, since agents need to claim larger portions of the limited total size.

Also we study $\Delta(t = T) - \ell$, which is how many sites are still available to agent 0 in the end of the simulation. This is a measure to estimate how large the role of confinement by their neighbors is. Small values indicate that the agents were limited by scent marks left by their neighbors, while large values indicate that there was still much territory unclaimed and the agent was limited by its diffusive character. In accordance with our observation that agents with smaller than typical territories are constrained by the small territory available, Fig. 9(b) shows that almost all agents in this category claim every last site. Similarly, agents with extremely large territories obtain them by not leaving sites unclaimed. Only in the region of typical instances we see realizations which leave significant portions of sites unclaimed. Overall, there is a high similarity of Fig. 9(a) and Fig. 9(b), which shows that rare realizations are mostly determined by rare initial positions of the agents, rather than by rare spatio-temporal evolutions.

IV. SUMMARY AND OUTLOOK

We studied a model for the emergence of territories by scent marks left by random walkers in one-dimension, which was used before to model the territorial behavior of foxes [17]. The typical, i.e., high-probability, behavior of our model turns out to be very different from the typical behavior of standard random walks. Using sophisticated large-deviation Markov chain Monte Carlo algorithms, we are able to obtain the distribution of the territory size over almost the full range of the support and many decades in probability. For the analysis, we concentrate on the behavior of extreme realizations, in which one individual either claims an extremely large or extremely small territory. The results indicate that the far right tail can be described by a rate function of a power law shape with exponent 2. This is similar to the behavior found for non-interacting random walks, which show that the presence of interactions, which lead to the emergence of territories, does not change the large-deviation behavior of the right tail substantially. This is also a good justification for the previous studies motivated by complex interacting systems to scrutinize the rare-event properties of simple models. Further, we use large parts of the joint probability densities of the territory size and the size of the largest adversarial territory or the size of unmarked territory, as well as examples of very atypical territory realizations to gain insight into the processes leading to atypical realizations.

For further studies in the rare-event range, it would probably not be very interesting to study the behavior as a function of the lifetime t_a of the scent. The reason is that for the present study with $t_a = \infty$ we already found an asymptotic similarity of these repelling, but not self-avoiding, random walks with the pure random

walk model. Nevertheless, it could be interesting to see whether this similarity still exists for larger dimensions than one. But for that purpose a much higher numerical effort would be needed.

[1] J. L. Brown and G. H. Orians, Annual Review of Ecology and Systematics **1**, 239 (1970).

[2] S. Harris, W. J. Cresswell, P. G. Forde, W. J. Trewhella, T. Woollard, and S. Wray, Mammal Review **20**, 97 (1990).

[3] B. J. Worton, Biometrics **51**, 1206 (1995).

[4] J. B. Karki, B. Pandav, S. R. Jnawali, R. Shrestha, N. M. B. Pradhan, B. R. Lamichane, P. Khanal, N. Subedi, and Y. V. Jhala, Oryx **49**, 150–156 (2015).

[5] N. Carter, S. Levin, A. Barlow, and V. Grimm, Ecological Modelling **312**, 347 (2015).

[6] C. O. Mohr, American Midland Naturalist **37**, pp. 223 (1947).

[7] F. Spitzer and H. Widom, Proc. Amer. Math. Soc. **12**, 506–509 (1961).

[8] S. N. Majumdar, A. Comtet, and J. Randon-Furling, Journal of Statistical Physics **138**, 955 (2010).

[9] J. Randon-Furling, S. N. Majumdar, and A. Comtet, Phys. Rev. Lett. **103**, 140602 (2009).

[10] M. Chupeau, O. Bénichou, and S. N. Majumdar, Phys. Rev. E **91**, 050104 (2015).

[11] D. S. Grebenkov, Y. Lanoiselée, and S. N. Majumdar, Journal of Statistical Mechanics: Theory and Experiment **2017**, 103203 (2017).

[12] G. Claussen, A. K. Hartmann, and S. N. Majumdar, Phys. Rev. E **91**, 052104 (2015).

[13] T. Dewenter, G. Claussen, A. K. Hartmann, and S. N. Majumdar, Phys. Rev. E **94**, 052120 (2016).

[14] H. Schawe, A. K. Hartmann, and S. N. Majumdar, Phys. Rev. E **96**, 062101 (2017).

[15] H. Schawe, A. K. Hartmann, and S. N. Majumdar, Phys. Rev. E **97**, 062159 (2018).

[16] H. Schawe and A. K. Hartmann, Journal of Physics: Conference Series **1290**, 012029 (2019).

[17] L. Giuggioli, J. R. Potts, and S. Harris, PLOS Computational Biology **7**, 1 (2011).

[18] J. R. Potts, S. Harris, and L. Giuggioli, PLOS ONE **7**, 1 (2012).

[19] A. K. Hartmann, *Big Practical Guide to Computer Simulations* (World Scientific, Singapore, 2015).

[20] H. Touchette, Physics Reports **478**, 1 (2009).

[21] J.-D. Deuschel and O. Zeitouni, Combinatorics, Probability and Computing **8**, 247 (1999).

[22] A. K. Hartmann, Phys. Rev. E **65**, 056102 (2002).

[23] H. Schawe and A. K. Hartmann, The European Physical Journal B **92**, 73 (2019).

[24] H. Chen, F. Huang, G. Li, and H. Zhang, arXiv preprint arXiv:1907.13330 (2019).

[25] M. Newman and G. Barkema, *Monte Carlo Methods in Statistical Physics* (Clarendon Press, 1999).

[26] N. Madras and G. Slade, "The self-avoiding walk," (Springer New York, New York, NY, 2013) Chap. Analysis of Monte Carlomethods, pp. 281–364.

[27] A. K. Hartmann, Phys. Rev. E **89**, 052103 (2014).

[28] N. Metropolis, A. W. Rosenbluth, M. N. Rosenbluth, A. H. Teller, and E. Teller, The Journal of Chemical Physics **21**, 1087 (1953).

[29] H. E. Daniels and F. Smithies, Mathematical Proceedings of the Cambridge Philosophical Society **37**, 244–251 (1941).

[30] B. D. Hughes, *Random walks and random environments* (Clarendon Press Oxford, 1996).

[31] A. Kundu, S. N. Majumdar, and G. Schehr, Phys. Rev. Lett. **110**, 220602 (2013).

[32] J.-S. Ferenc and Z. Néda, Physica A: Statistical Mechanics and its Applications **385**, 518 (2007).